J. Mater. Environ. Sci. 5 (5) (2014) 1426-1433
ISSN : 2028-2508
CODEN: JMESCN

Photocatalytic degradation of rhodamine B using nanocrystalline α-Fe_2O_3

A.A. Jahagirdar[a], M.N. Zulfiqar Ahmed[b*], N. Donappa[c], H. Nagabhushana[d]
B.M. Nagabhushana[e]
[a]*Department of Chemistry, Dr. Ambedkar Institute of Technology, Bangalore, India.*
[b]*Department of Chemistry, HKBK College of Engineering, Bangalore, India.*
[c]*Department of Chemistry, Maharani Lakshmi Ammanni College for Women, Bangalore, India.*
[d]*Department of P.G. Studies and Research in Physics, Tumkur University, Tumkur, India.*
[e]*Department of Chemistry, M.S. Ramaiah Institute of Technology, Bangalore, India.*

Received 10 Mar 2013; Revised 23 May 2014; Accepted 23 May 2014

** Corresponding author. E-mail: zulfi_chem@yahoo.com*

Abstract

Nanocrystalline α-Fe_2O_3 was synthesized by solution combustion method. The as-formed α-Fe_2O_3 nanopowder was characterized by Powder X-ray diffraction (PXRD), Scanning electron microscopy (SEM) and Fourier transform infrared spectroscopy (FTIR). The as-formed nanopowder was used as photocatalyst for the degradation of the dye rhodamine B (RhB) under ultraviolet (UV) light illumination. The effects of pH, amount of the photocatalyst, amount of H_2O_2 and irradiation time were studied. It was found that nanocrystalline α-Fe_2O_3 acts as an efficient photocatalyst for the degradation of RhB in presence of H_2O_2 under UV light. At pH 10, in presence of H_2O_2 and UV light, maximum degradation of RhB was achieved for a catalyst dosage of 0.8g of the catalyst per liter of the dye solution in just 40 minutes.

Keywords: Solution combustion, Photodegradation, Rhodamine B, SEM, nanopowder.

1. Introduction

Among the several hazardous compounds that are found in water, dyes are an important class of concern. The treatment of colored wastewater not only involves its decolorization, but also its detoxification [1]. Textile and similar other industries release large amounts of colored dye effluents into the water. These dye effluents are toxic and many of them are non-biodegradable. These effluents create major environmental problems and release potentially harmful carcinogenic substances in water [2-5]. A number of physical and chemical treatment processes including precipitation, adsorption, air stripping, flocculation, reverse osmosis and ultrafiltration are being employed for the removal of these toxic pollutants from water. Most of these methods suffer from various drawbacks [6-9].

Photocatalysis is being considered as an efficient process for the mineralization of toxic organic compounds, hazardous inorganic constituents and bacterial disinfection due to the generation of hydroxyl radicals ($OH^{\bullet}$) which possess strong oxidizing potential [10-12]. Metal oxide semiconductors such as zinc oxide (ZnO), titanium dioxide (TiO_2), ferric oxide (α-Fe_2O_3), tungsten oxide (WO_3) etc. have been considered as dynamic photocatalysts since they promote photocatalysis upon illumination with ultraviolet (UV) light. An efficient semiconductor should have high optical stability, high sensitivity for UV-Visible light and low fabrication cost [13]. Most of the semiconductors have band gaps in the UV region and hence promote photocatalysis upon illumination with UV light. α-Fe_2O_3 is highly stable and an inexpensive photocatalyst. It is resistant to photocorrosion and is environmental friendly. As a result of these properties, nanocrystalline α-Fe_2O_3 has been widely used as photocatalyst by many researchers. Many methods are employed in the synthesis of nano metal oxides such as co-precipitation, sol-gel, microemulsion, hydrothermal, combustion pyrolysis and ultrasonic assisted methods. Most of these methods suffer from one or the other draw back such as long reaction times, requirement of high temperature etc. [14-16]. In the present work, nanocrystalline α-Fe_2O_3 was prepared by solution combustion method. It is an easy and versatile method which requires comparatively lower temperature and lesser time duration. The as-formed α-Fe_2O_3 nanopowder was used in the photocatalytic degradation of rhodamine B (RhB) dye. The results indicated that nanocrystalline α-Fe_2O_3 is an efficient photocatalyst for the degradation of RhB dye in presence of H_2O_2 and ultraviolet light.

2. Materials and methods

2.1.1 Chemicals used

Ferric nitrate and rhodamine B (RhB) were obtained from sd Fine Chemicals Limited. Ferric nitarate was used as oxidizer and oxalyl dihydrazide (ODH) was used as fuel. The fuel ODH was prepared by the method described elsewhere [17]. 1000 ppm stock solution of RhB dye was prepared as the stock solution. The stock solution was appropriately diluted with distilled water to give solution of concentration 20 ppm. All the reagents were of analytical grade and were used without purification. Distilled water was used throughout the experiment.

2.1.2 Preparation of α- Fe2O3 nanopowder

An aqueous solution containing stoichiometric amounts of ferric nitrate, Fe $(NO_3)_3.9H_2O$ and ODH, $C_2H_6N_4O_2$ was taken in a petridish of approximately 300 ml capacity. The solution was heated over a hot plate until the excess water was evaporated. The petridish was then introduced into a muffle furnace maintained at 300 ± 10^o C. The reaction mixture undergoes thermal dehydration and ignites at one spot with the liberation of gaseous products such as oxides of nitrogen and carbon. The combustion process propagates throughout the reaction mixture without further need of any external heating, as the heat of the reaction is sufficient for the decomposition of the redox mixture. The flame temperature was found to be around 1200°C, as measured by a thermocouple placed inside the petridish without touching the solution.

2.2 Characterization of the photocatalyst

The as-formed α-Fe_2O_3 was characterized by Powder X-ray diffraction (PXRD), Fourier transform infrared spectroscopy (FTIR) and Scanning electron microscopy (SEM).

2.2.1 Powder X-ray diffration (PXRD)

The phase purity and crystallinity of the as-formed α-Fe_2O_3 nanopowder was determined by powder X-ray diffraction studies (PXRD). The measurements were performed on a Philips X-ray diffractometer (PW/1050/70/76) using Cu Kα radiation (λ = 1.542 Å) at 30 kV and 20 mA with Ni filter.

2.2.2 Fourier transform infrared spectroscopy (FTIR)

The various modes of vibration of the nanopowder were determined by Fourier transform infrared spectroscopy. The FTIR spectrum of the as-formed α-Fe_2O_3 nanopowder was recorded using Nicollet IMPACT 400 D FTIR spectrometer from 4000 to 300 cm^{-1} using KBr as the reference sample.

2.2.3 Scanning electron microscopy (SEM)

The morphology of the as-formed α-Fe_2O_3 nanopowder was determined by scanning electron microscopy. The SEM images were recorded using JEOL (JSM-840A) scanning electron microscope.

2.3 Photocatalytic experiments

Rhodamine B is used as a dye in the textile industries. Chemically, it is [9-(2-carboxyphenyl)-6-diethylamino-3-xanthenylidene]-diethylammonium chloride. It is toxic and soluble in water, methanol and ethanol. It is often used as a tracer dye within water to determine the rate and direction of flow and transport. Rhodamine dyes can thus be detected easily and inexpensively with an instrument called fluorometer. Rhodamine dyes are used extensively in biotechnology applications such as fluorescence microscopy, flow cytometry and fluorescence correlation spectroscopy. The chemical structure and absorption spectrum of RhB are shown in the figures 1 and 2 respectively. It shows maximum absorption at 556 nm.

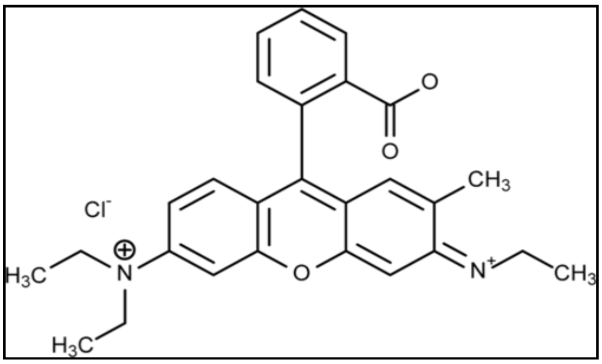

Figure 1 Structure of RhB dye

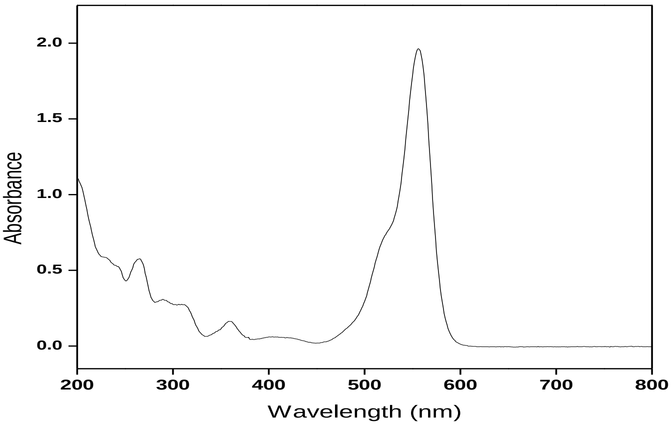

Figure 2 Absorbance spectrum of RhB

Prior to photocatalytic experiments, studies were carried out by transferring 50 mL of the 20 ppm dye solution into the photoreactor. 100 mg of the photocatalyst was added to it and the suspension was stirred magnetically in the dark for about 30 minutes. The solution was then centrifuged at 3000 rpm for 10 minutes using Remi C8C centrifuge and the UV-Visible spectrum was recorded from 190 to 800 nm using ELICO SL-159 UV-Visible spectrophotometer. It was found that there was negligible degradation of the dye under dark conditions.

The photocatalytic experiments were carried out in a reaction cell of circumference 25.2 cm and 500 mL capacity with the exposure area of 50.3 cm^2. A 125 watt mercury vapor lamp was used as the source of UV light. The distance between the surface of the solution and the mercury lamp was 20 cm. 50 ml of the dye solution was transferred into the reaction vessel and appropriate amounts of the photocatalyst and H_2O_2 were added to it. The solution was magnetically stirred under UV light for 30 minutes. The solution was then filtered and centrifuged at 3000 rpm for 10 minutes and the UV-Visible spectrum was recorded as described earlier.

2.3.1 Effect of pH

Waste water containing dyes is discharged at different pH. Therefore it is important to study the effect of pH on decoloration of the dye. The pH affects not only the surface properties of the photocatalyst, but also the dissociation of the dye molecules and formation of hydroxyl radicals. In the present study, the effect of pH of the solution on the photocatalytic degradation of RhB was examined ranging from pH 2 to 12.

2.3.2 Effect of dosage of photocatalyst

The effect of amount of photocatalyst on the degradation of RhB dye was carried out by varying the amount of photocatalyst from 0.2 to 2.0 g per liter of the dye solution.

2.3.3 Effect of H_2O_2

H_2O_2 is one of the strong oxidizing agents used in the degradation of azo dyes. In the present study, the effect of H_2O_2 was studied by varying the amount of H_2O_2 from 0.1 to 1.0 mL per liter of the dye solution.

2.3.4 Effect of irradiation time

The effect of irradiation time on the rate of photocatalytic degradation of RhB was studied after selecting the optimum dosage of the photocatalyst and the optimum amount of H_2O_2. The irradiation time was varied from 5 to 60 minutes with intervals of 5 minutes. 50 ml of the dye solution containing optimum amounts of the photocatalyst and H_2O_2 was exposed to UV light at room temperature. After every 5 minutes, a small aliquot of the sample was withdrawn, centrifuged and the UV-Visible spectra were recorded for each sample.

3. Results and DISCUSSIONS

3.1 Powder X-ray DIFFRACTION (PXRD)

Figure 3 shows the PXRD pattern of as-formed α-Fe_2O_3 nanopowder. All the diffraction peaks are in good agreement with those of the standard patterns of the rhombohedral phase of α-Fe_2O_3 (JCPDS file number: 87-1165) with a = 5.035 Å, c = 13.749 Å. The diffracted patterns are well matching with the literature [18]. The diffraction peaks of the sample are well defined revealing the well-crystalline character of the sample. No peaks of other phases and impurities were defined. The mean crystallite size as calculated by applying Scherer's formula to the full width at half maximum (FWHM) was found to be around 44 nm.

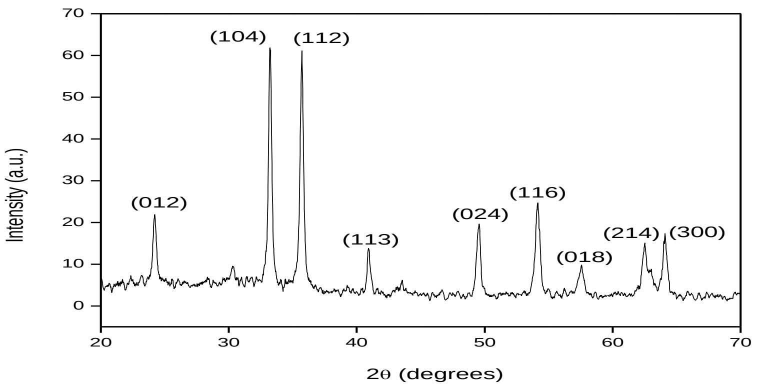

Figure 3 PXRD pattern of Fe_2O_3 nanopowder

3.2 Fourier transform infrared spectroscopy (FTIR)

Figure 4 shows the FTIR spectrum of the α-Fe_2O_3 nanopowder. The peaks at around 446 and 533 cm^{-1} correspond to the characteristic vibrations of the Fe-O bond [19]. The absorption peak at 3433 cm^{-1} corresponds to the –OH group of water absorbed on the surface of the nanopowder.

3.3 Scanning electron microscopy (SEM)

For combustion method it is well known that the morphological characteristics of the prepared powder are strongly dependent on the heat and gases generated during the complex decomposition. Large amount of gases are suitable for preparation of tiny particles while the heat released is an important factor for crystal growth. Figure 5 shows the SEM micrograph of the as-formed α-Fe_2O_3 nanopowder. It is observed that the particles are agglomerated and have irregular shape.

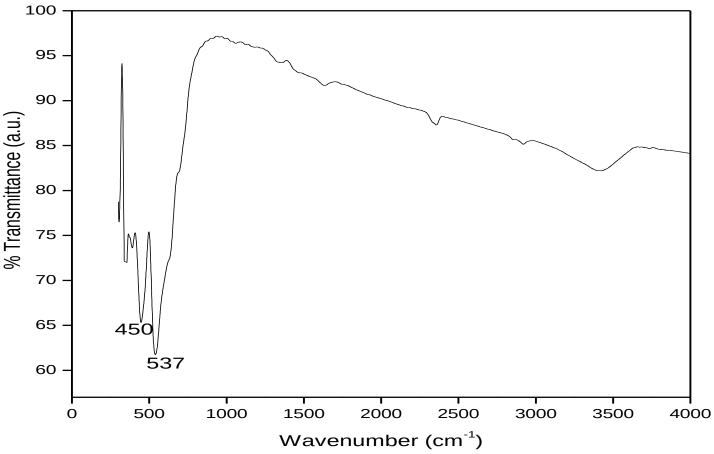

Figure 4 FTIR spectrum of α-Fe_2O_3 nanopowder

The agglomeration of nanoparticles is usually explained as a common way to minimize their surface free energy; however some workers say that agglomeration is assigned to the presence of organic radicals that act as binders. The voids and pores present in the sample are due to large amount of gases produced during the combustion synthesis.

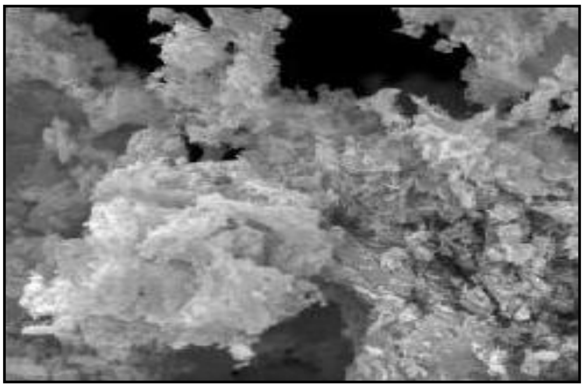

Figure 5 SEM micrograph of α-Fe_2O_3 nanopowder

3.4 Effect of pH

Figure 6 shows the effect of pH on the photocatalytic degradation of RhB by the photocatalyst. It was observed that the photocatalytic degradation was effective at pH 10. Hence pH 10 was considered as the optimum pH. This can be attributed to the increase of hydroxyl ions, which induce more hydroxyl radical formation.

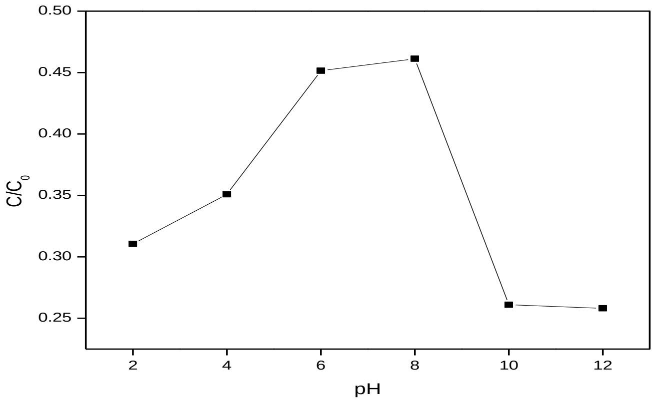

Figure 6 Effect of pH

3.5 Effect of dosage of photocatalyst

Figure 7 shows the effect of dosage of photocatalyst on the photocatalytic degradation of RhB. It was observed that maximum degradation of the dye occurred at a dosage of 1 g of the photocatalyst per liter of the dye solution (90.13 % degradation). Beyond this dosage, the degradation was found to be negligible. This can be explained as follows. As the amount of photocatalyst increases, the number of dye molecules adsorbed will increase and the number of photons absorbed also increases. As a result of this high density of molecules in the area of illumination, the rate of photodegradation increases. However, for very high catalyst dosage, the suspension's turbidity increases. In such a situation, the light penetration decreases. As a result of this, there is an enhancement in light scattering and consequently the photodegradation process will be less effective.

The degradation efficiency is given by equation 1:

$$Degradation\ efficiency = \frac{C_o - C}{C_o} \times 100 \qquad (1)$$

where, C_o = initial dye concentration and C = dye concentration after degradation.

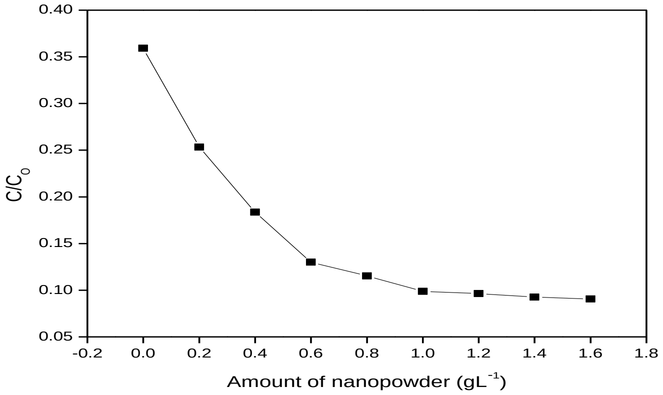

Figure 7. Effect of dosage of photocatalyst

3.6 Effect of H2O2

Figure 8 shows the effect of H_2O_2 on the photocatalytic degradation of RhB. It was observed that the degradation was maximum for 0.5 mL of H_2O_2 per liter of the dye solution. The mechanism for the photocatalytic degradation of RhB under UV/H_2O_2/α-Fe_2O_3 system can be explained as follows. In the presence of the photocatalyst, H_2O_2 absorbs UV light and undergoes homolytic cleavage leading to the generation of hydroxyl free radicals (${}^{\cdot}$OH). These hydroxyl free radicals get adsorbed on the surface of the photocatalyst thus degrading the dye molecules as shown below.

$$H_2O_2 + e \rightarrow \bullet OH + OH^-$$
$$\bullet OH + H_2O_2 \rightarrow H_2O + HO_2\bullet$$
$$\bullet OH + HO_2\bullet \rightarrow H_2O + O_2$$
$$OH^{\bullet\cdot} + \text{dye molecule} \rightarrow \text{Intermediates} \rightarrow CO_2\uparrow + H_2O + \text{mineral salts.}$$

The photocatalytic reaction may be considered to take place by the one represented by the following mechanism. In the Fe^{3+} / H_20_2 / UV system, the photolysis of Fe^{3+} primarily leads to the production of $OH^{\bullet}$ radicals and Fe^{2+}. Moreover, $OH^{\bullet}$ radicals are also produced by photolysis of H_20_2 and by the reaction of H_20_2 with Fe^{2+}.

$$Fe_2O_3 + h\upsilon \rightarrow Fe_2O_3^*$$
$$Fe_2O_3^* + H_2O \rightarrow Fe_2O_3^* + H^+ + OH^{\bullet}$$
$$OH^{\bullet\cdot} + \text{dye molecule} \rightarrow \text{Intermediates} \rightarrow CO_2\uparrow + H_2O + \text{mineral salts.}$$

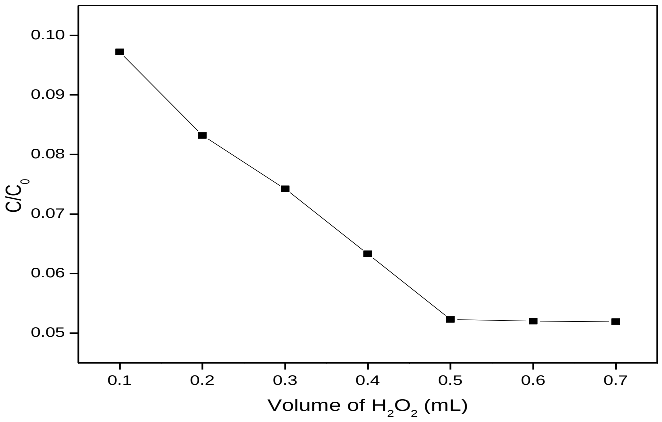

Figure 8 Effect of H_2O_2

3.7 Effect of irradiation time

Figure 9 shows the effect of irradiation time on the photocatalytic degradation of RhB. It was observed that maximum degradation of the dye occurred in just 40 minutes of irradiation. Beyond 40 minutes, the degradation was found to be negligible. From the results obtained it can be concluded that the photocatalytic approach promotes the decline of chromophore peaks in the dye molecule in 40 minutes reflecting that the de-ethylation of RhB is the main reaction occurring at the surface.

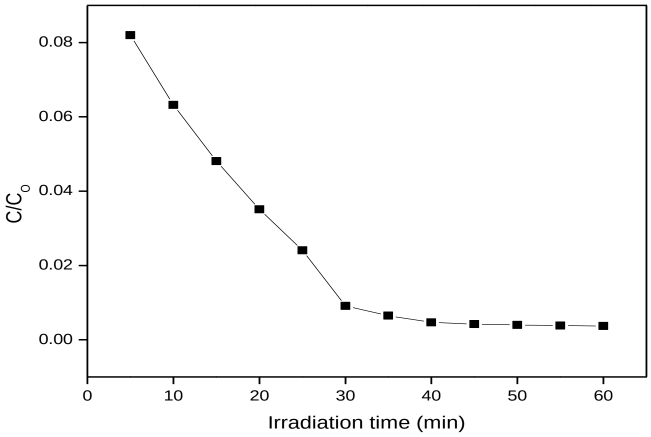

Figure 9 Effect of irradiation time

Conclusions

Nanocrystalline α-Fe_2O_3 was synthesized by solution combustion method. The as-formed nanopowder was characterized by PXRD, SEM and FTIR. The nanopowder was used as photocatalyst for the degradation of Rhodamine B dye. The results indicated that the photocatalytic activity of α-Fe_2O_3 was greatly enhanced in presence of H_2O_2 and UV light at a pH of 10. This indicates that α-Fe_2O_3 can be used as a potential photocatalyst in the treatment of wastewater from textile mills and other similar industries

Acknowledgements-The authors are thankful to the TEQIP laboratory of MSRIT, Bangalore for providing facilities to carry out the experimental work. AAJ is thankful to the Principal and management of Dr. AIT, Bangalore for encouragement and support. MNZA is thankful to the Principal and management of HKBKCE, Bangalore for encouragement and support.

References

1. Agatino Di Paola, Elisa García-López, Giuseppe Marcì, Leonardo Palmisano, *Journal of Hazardous Materials B.* 211-212 (2012) 3.
2. Vinod Gopal, K., Kamat, P.V., *Environ. Sci. Technol.* 29 (1995) 841.
3. Ho Chang, Tsing Tshin Tsung, Hong-Ming Lin, Chung-Kwei Lin, *China Particuology*. 2 (4) (2004) 171.
4. Amany S. Youssef, Mervat F. El-Sherif, Samy A. El-Assar, *Biotechnology*. 7 (2008) 213.
5. Syed Abu Sayeed Mohammed, Maya Naik, *J. Environ. Sci. Tech.* 4 (2011) 504.
6. Arslan I, Balcioglu IA, Bahnemann DW, *Dyes and Pigments*. 47**(**3) (2000) 207.
7. S.K. Kansal, M. Singh, D. Sud, *Journal of Hazardous Materials*, 141 (2007) 581–590.
8. Hayat, K., Gondal, M.A., Khaled, M.M., Yamani, Z.H., Ahmed, S., *J. Hazard. Mater.* 186 (2-3) (2011) 1226.
9. Ramalakshmi, S., Muthuchelian, K., Swaminathan, K., *J. Environ. Sci. Tech*. 5 (2012) 222.
10. Jeanette M.C. Robertson, Peter K. J. Robertson, Linda A. Lawton, *J. Photochem. Photobio. A: Chemistry*. 175 (1) (2005) 51.
11. Fatimah I., Shukla P.R., Kooli, F., *J. App. Sci.* 9 (2009) 3715.
12. Kavitha, S.K., Palanisamy, P.N., *Modern App. Sci.* 4 (2010) 190.
13. Olugbenga Solomon Bello, Mohammed Azmier Ahmad, Tan Tong Siang, *Trends in App. Sci. Res.* 6 (2011) 794.
14. Gupta, G.S., Prasad, G., Singh, V. N., *Water Res*. 24 (1990) 45.
15. Pagga, U., Taeger, K., *Water Res*. 28 (1994) 1051.
16. Pramod H. Borse, Cho, C. R., Lim, K. T., Bae, J. S., Jeong, E. D., Hong, T. E., Kim, H. J., Kim, H. G., *J. Cer. Pro. Res.* 12 (5) (2011) 592.
17. Patil, K.C., Hegde, M. S., Tanu Rattan, Aruna, S.T., Chemistry of Nanocrystalline Oxide Materials: Combustion Synthesis, Properties and Applications, World Scientific, 2008.
18. Hua, J., Gengsheng, J., *Mater. Lett.* 63 (2009) 2725.
19. Jahagirdar, A. A., Zulfiqar Ahmed, M. N., Donappa, N., Nagabhushana, H., Nagabhushana, B. M., *Trans. Ind. Ceram. Soc*, **70 (3)** (2011) 71.